Supplementary Information for "Electrically mediated self-assembly and manipulation of drops at an interface"

Paul R. Kaneelil,[1] J. Pedro de Souza,[2] Günther Turk,[3] Amir A. Pahlavan,[4] and Howard A. Stone[1]

[1] *Department of Mechanical and Aerospace Engineering, Princeton University, Princeton, New Jersey 08544, USA*
[2] *Omenn-Darling Bioengineering Institute, Princeton University, Princeton, New Jersey 08544, USA*
[3] *Princeton Materials Institute, Princeton University, Princeton, New Jersey 08544, USA*
[4] *Department of Mechanical Engineering and Materials Science, Yale University, New Haven, Connecticut 06511, USA*

(Dated: June 10, 2024)

I. CHARGE OF THE DROPS

In all the experiments for configuration 2, we used the same protocol the create the drops to ensure that the drops are uniformly charged (see Methods section). Since the charging relies on contact charge separation, which can be irregular compared to a more controlled method using electrodes and high voltages, we note that the drops may not be charged the exact same amount. We measured the charge of the drops using a Faraday cup and a NanoCoulomb meter (Monroe Electronics; Model 284). Figure S1 shows the charge of the drops as they were sequentially dispensed into the Faraday cup. The error bars represent the inaccuracy of the measurement. On average, the drops had a charge of $Q_d = 0.07 \pm 0.01$ nC.

II. ELECTROSTATIC MODEL

We derive a simplified theoretical model to elucidate the dependence of the collective behavior of the drops on the bath height h. Consider the geometry shown in Fig. 3(e) in the main text, where the drop is assumed to be a flat circle of radius R located at the origin with a uniform charge distribution. We consider a domain that is infinite in the radial direction r and semi-infinite in the axial direction z, where there is a finite height h of oil below the drop with a relative permittivity ϵ_r and an infinite layer of air above the drop. The electrostatic potential ϕ for this axisymmetric system satisfies the Laplace equation

$$\nabla^2\phi = \frac{1}{r}\frac{\partial}{\partial r}\left(r\frac{\partial\phi}{\partial r}\right) + \frac{\partial^2\phi}{\partial z^2} = 0. \tag{S1}$$

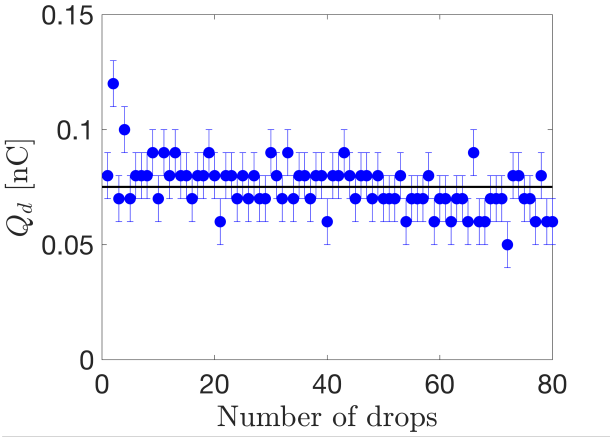

FIG. S1. The charge of the drops as measured using a Faraday cup and a NanoCoulomb meter. The error bars represent the measurement error and the solid black line represents the average of the data.

in both the air phase ($z > 0$) and the oil phase ($z < 0$). The boundary conditions in the z-direction specifies a vanishing electric field far away from the drop, a jump in the field at the interface, and a vanishing potential at the conductive lower boundary:

$$\frac{\partial \phi}{\partial z}(r, z \to \infty) = 0, \tag{S2a}$$

$$\frac{\partial \phi}{\partial z}(r, z = 0^+) - \epsilon_r \frac{\partial \phi}{\partial z}(r, z = 0^-) = -\frac{q_d}{\epsilon_0}\, \mathcal{H}(R - r), \tag{S2b}$$

$$\phi(r, z = -h) = 0. \tag{S2c}$$

Here, $\epsilon_0 = 8.854 \times 10^{-12}$ F/m is the permittivity of free space, q_d is the charge per area on the drop, and $\mathcal{H}$ is the Heaviside step function. The boundary conditions in the r-direction specifies symmetry at the center and a vanishing electric field far away:

$$\frac{\partial \phi}{\partial r}(r = 0, z) = 0, \tag{S3a}$$

$$\frac{\partial \phi}{\partial r}(r \to \infty, z) = 0. \tag{S3b}$$

Taking advantage of the circular symmetry and to readily satisfy the boundary conditions in the r-direction, we use the Hankel transform to solve Eqs. S1 - S3. The Hankel transform of ϕ, represented by the transformed variable $\Phi(k, z)$, and the inverse transform are defined as

$$\Phi(k, z) = \int_0^\infty \phi(r, z)\; J_0(kr) r\, dr, \tag{S4a}$$

$$\phi(r, z) = \int_0^\infty \Phi(k, z)\; J_0(kr) k\, dk \tag{S4b}$$

where J_0 is the Bessel function of the first kind of order zero and k is the transformed independent variable.

The transformed Eq. S1 becomes $\frac{\partial^2 \Phi}{\partial z^2} - k^2 \Phi = 0$. After satisfying the boundary conditions, the solution is

$$\Phi(k, z) = \begin{cases} A(k)\; e^{-kz}, & z \geq 0 \\ B(k)\; \sinh[k(z + h)], & z \leq 0 \end{cases} \tag{S5}$$

where $A(k) = \frac{Q(k)\; \sinh(kh)}{k\epsilon_0[\epsilon_r \cosh(kh) + \sinh(kh)]}$, $B(k) = \frac{Q(k)}{k\epsilon_0[\epsilon_r \cosh(kh) + \sinh(kh)]}$, $Q(k) = \frac{Q_d}{\pi k R} J_1(kR)$, and Q_d is the total charge on the drop.

The inverse transform integral does not have a closed form analytical solution. But, we can approximate the integral analytically and calculate the pair potential at the interface, $z = 0$, at two relevant limits. When the bath is deep $kh \to \infty$, and the drop is small $kR \to 0$ compared to the separation between two drops, i.e. $h/r \to \infty$, we get

$$\phi_1(r, z = 0) \approx \frac{Q_d}{4\pi\epsilon_0 r}\left(\frac{2}{\epsilon_r + 1}\right). \tag{S6}$$

In this limit, the potential is independent of the height of the bath. Conversely, when the height of the bath and the size of the drop are small compared to the separation between two drops, $kh \to 0$ and $kR \to 0$, i.e. $h/r \to 0$, we get

$$\phi_2(r, z = 0) \approx \frac{2Q_d h^2}{4\pi\epsilon_0 \epsilon_r^2 r^3}. \tag{S7}$$

In this limit, the potential has a quadratic dependence on the height of the oil bath. Notice also that the potential has an inverse square dependence on the dielectric constant of the oil bath, which explains why the electrostatic interactions and self-assembly are not seen when using an oil with large ϵ_r. These approximations also assume that the drop is a point charge ($kR \to 0$). In Fig. S2(a)-(d), we plot the exact solution and the two approximations for four different h/R values. Note that non-dimensionalizing the length with R artificially introduces R back into the two approximations. This is done simply to plot all the solutions together which reveals more insight: the deep bath approximation (red dashed-dotted line) agrees with exact solution around the vicinity of the drop ($r/R = 1$) as h/R increases, whereas the shallow bath approximation (blue dashed line) agrees with the exact solution farther away from the drop ($r/R \gg 1$) as h/R increases.

We also note that the full potential at the interface $\phi(r, z = 0)$ can be approximately represented as the scaled Harmonic mean of the two limits as, $\phi_m \approx 1/2\; H(\phi_1, \phi_2) = (1/\phi_1 + 1/\phi_2)^{-1}$, and is given in Eq. 1 in the main text. While ϕ_m (green dotted line) is built on the point charge assumption, we see that it agrees well with the exact solution ϕ for finite R, as shown in Fig. S2. This agreement seems to only hold for small relative permittivity, namely $\epsilon_r < 2$. We use the analytical form ϕ_m to make quantitative comparison between the theory and the experiments.

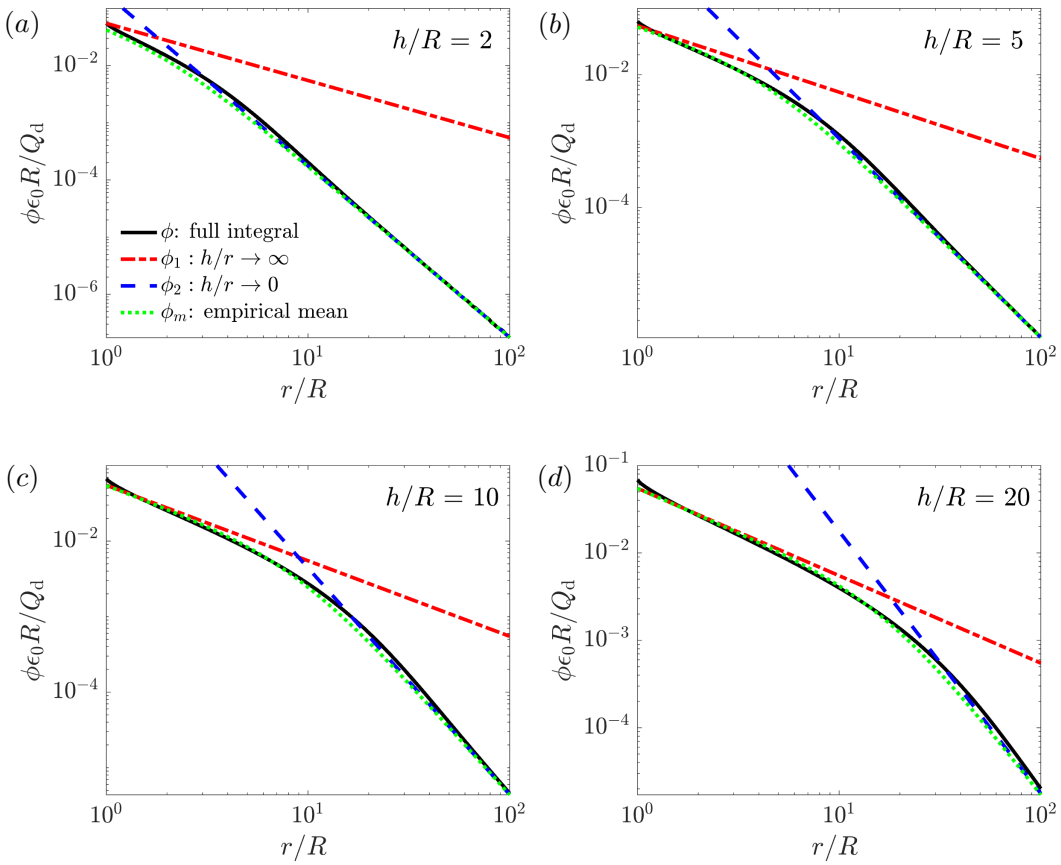

FIG. S2. The theoretical electric potential near a drop. The black line is the exact solution from the integral in Eq. S4b, the red dashed-dotted line corresponds to the deep bath limit from Eq. S6, the blue dashed line corresponds to the shallow bath limit from Eq. S7, and the green dotted line corresponds to the empirical mean from Eq. 1 in the main text. We plot the solutions for four different values of dimensionless bath height: (a) $h/R = 2$, (b) $h/R = 5$, (c) $h/R = 10$, and (d) $h/R = 20$.

III. ENERGY OF THE DROPS AT THE INTERFACE

The total energy of a pair of drops interacting at the oil-air interface might include a contribution from the capillary interactions and the electrostatic interactions. In this section, we compare the strength of these interactions to show that our experimental system with charged drops is dominated by electrostatic repulsion. Assuming the capillary interactions are similar to that of particles at an interface [1], the total energy can be written as follows:

$$U(r) = -2\pi\gamma R^2 Bo^2 \Sigma^2 K_0(r/l_c) + \frac{Q_d^2 h^2}{2\pi\epsilon_0 r[(\epsilon_r+1)h^2 + \epsilon_r^2 r^2]}, \tag{S8}$$

where $\Sigma = \left(\frac{2D-1}{3} - \frac{1}{2}\cos(\theta) + \frac{1}{6}\cos^3(\theta)\right)$, $D = \rho_w/\rho_o$ is the density ratio of water to oil in this case, $Bo = \rho_o g R^2/\gamma$ is the bond number, $l_c = \sqrt{\gamma/(\rho_o g)}$ is the capillary length, and K_0 is the modified Bessel function of the second kind of order zero. The first term in Eq. S8 is valid for $Bo \ll 1$, whereas $Bo = 2.4$ in our experiments. The larger Bo in our experiments means that the shape of the oil-air interface near the water drop is more complex. However, it is still fair to assume that the deformation of the interface is of $\mathcal{O}(l_c)$ [2]. Thus, this analysis will still yield correct order of magnitude estimates although it is quantitatively imprecise. We rescale the equation such that $\overline{U} = U/U_c$ and $\overline{r} = r/l_c$, to get

$$\overline{U}(\overline{r}) = -AK_0(\overline{r}) + \frac{1}{\overline{r}^3 + B\overline{r}}, \tag{S9}$$

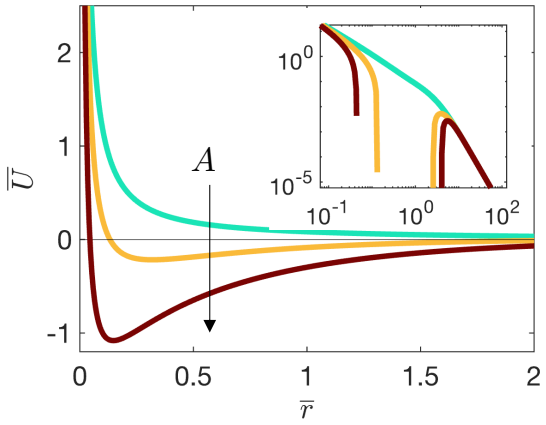

FIG. S3. The dimensionless total energy represented by Eq. S9 with $A = 0.1,\ 0.5$, and 1 for green, yellow, and brown colored lines, respectively, and $B = 7$.

where $U_c = \frac{Q_d h^2}{2\pi\epsilon_0\epsilon_r^2 l_c^3}$, $A = \frac{4\pi^2\gamma R^2 Bo^2\Sigma^2\epsilon_0\epsilon_r^2 l_c^3}{Q_d^2 h^2}$, and $B = \frac{(\epsilon_r+1)h^2}{\epsilon_r^2 l_c^2}$. Note that both the capillary and electrostatic interactions are derived based on the assumption that the potentials can be superposed, neglecting non-linear effects. The equilibrium distance $\overline{r}_{eq} = \overline{\ell}_{eq} = \ell_{eq}/l_c$ between the drops correspond to the minimum energy state that must satisfy $\frac{d\overline{U}}{d\overline{r}} = 0$. However, we find that this condition does not predict the experimental results. In other words, the total energy in Eq. S9 does not have a local minimum, as shown in Fig. S3, at experimentally relevant values of $A \approx 0.1$ and $B \approx 7$. If A is slightly larger, a local minimum starts to appear at $\ell_{eq}/l_c = \mathcal{O}(0.1)$ or smaller. But, the quasi-equilibrium distances observed in experiments are about two orders of magnitude larger: $\ell_f/l_c = \mathcal{O}(10)$. This discrepancy suggests that the interactions between the drops are dominated by electrostatic repulsion and that the system indeed is not in equilibrium within the observation time in experiments. The drops must be continually repelling and moving away from each other.

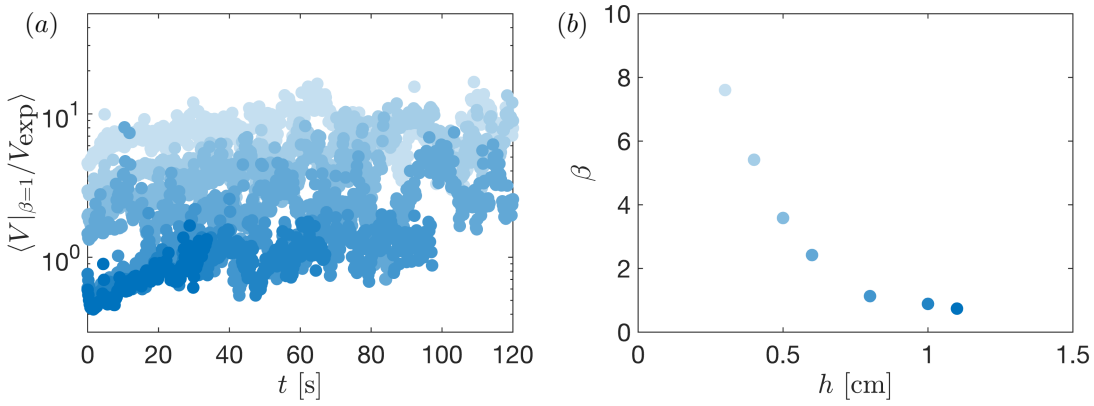

FIG. S4. The fitting parameter β. (a) $\langle V|_{\beta=1}/V_{\rm exp}\rangle$ as a function of t before finding the value of β shows that the data sets are not all clustered around unity. (b) The fitting parameter β as a function of the height of the oil bath h.

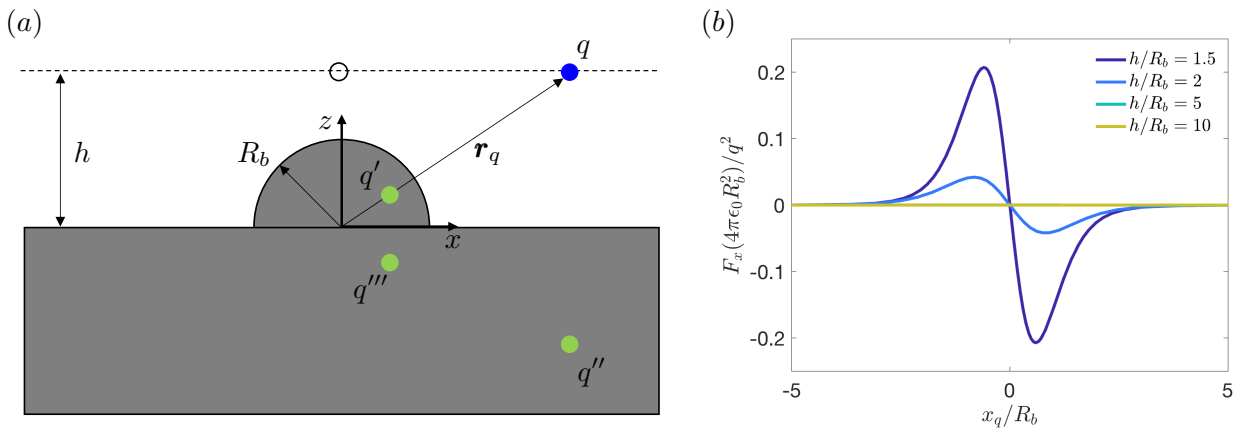

FIG. S5. The hemispherical boss. (a) Schematic of the hemispherical boss shape studied in a model, where a point charge q is restricted to be at a height $z = h$. The image charges are shown as green circles. The force-free point directly above the boss, where the distance between the charge q and the conductor becomes minimal, is indicated by an open circle. (b) The x-component of the theorerical force on a charge q in the hemispherical boss configuration for various h/R_b values.

IV. FITTING PARAMETER

Balancing viscous stresses and electrostatic repulsion, we showed that the theoretical velocity of the charged drop as it repels another can be modelled as $\mathbf{V} = -\frac{Q_d}{6\beta\pi\mu_o R}\frac{d}{dr}[\phi_m(r, z = 0)]$, where β is a fitting parameter that accounts for any excess drag due to the presence of the interface and the bottom surface of the container in shallow cases. In Fig. S4(a), we show $\langle V|_{\beta=1}/V_{\text{exp}}\rangle$ where β is simply set to 1. The value of β was then calculated such that the mean of $\langle V/V_{\text{exp}}\rangle$ became unity for each data set.

For a solid particle at a fluid-fluid interface, it has been shown that β is a function of the contact angle that the interface makes with the particle [3]. In our case, the drop might always have a layer of oil above it so there might not even be a contact angle. While we have not verified this directly, it could be the reason why β is almost 1 at large h, suggesting to a first approximation that the drop is simply moving within the oil phase.

But, we believe the largest effect on the drag experienced by the drop might be from the lubricating layer below the drop in shallow bath cases. In Fig. S4(b) we report the values of β used to fit the experimental results to the model in Fig. 3(g) in the main text. We note that $\beta \approx \mathcal{O}(1)$ in all cases. Note that we go down to $h = 3$ mm, which is about the diameter of the drop. As h decreases, the drop gets closer to the wall and β increases. This trend is consistent with theoretical predictions that shows that lubrication effects enhances the drag of a particle moving next to a wall, as a function of the distance from the wall [4].

V. THE HEMISPHERICAL BOSS

As discussed in the main text, we analyze the electrostatic effect that drives the drops towards shallow regions above a conductor qualitatively by considering the textbook example of a point charge q near a conducting plane with a hemispherical boss of radius R_b [5], as shown in Fig. S5(a). Taking into account that the charged drop is confined to the surface of the suspending oil bath, the point charge is restricted to be at a height $z = h$ above the conducting plane. With respect to the center of the hemispherical boss, the position vector of the charge is then $\mathbf{r}_q = (x_q, 0, h)^T$. Using a method of images it can be shown that in the x-direction a force acts on the charge with the magnitude

$$F_x = F_x^\circ + \frac{q^2}{4\pi\epsilon_0}\frac{R_b}{r_q}\left(1 - \frac{R_b^2}{r_q^2}\right)\left[x_q^2\left(1 - \frac{R_b^2}{r_q^2}\right)^2 + h^2\left(1 + \frac{R_b^2}{r_q^2}\right)^2\right]^{-\frac{3}{2}} x_q, \tag{S10}$$

where we have defined the force F_x° on a point charge due to a sphere of radius R_b centered at the origin,

$$F_x^\circ = -\frac{q^2}{4\pi\epsilon_0}\frac{R_b}{r_q^4}\left(1-\frac{R_b^2}{r_q^2}\right)^{-2} x_q. \tag{S11}$$

It is then easy to see that the charge is forced towards $x_q = 0$, where the force in x-direction vanishes. This is the point where the distance between the charge and the conductor becomes minimal. Equation S10 is plotted in Fig. S5(b) in a non-dimensional form for various non-dimensional height h/R_b. Notice that the force vanishes at $x_q/R_b = 0$ for small h/R_b, and that the force becomes independent of position as h/R_b increases, as expected.

---

[1] B. Majhy, S. Jain, and A. Sen, Attraction and repulsion between liquid droplets over a liquid-impregnated surface, The Journal of Physical Chemistry Letters **11**, 10001 (2020).

[2] I. Ho, G. Pucci, and D. M. Harris, Direct measurement of capillary attraction between floating disks, Physical Review Letters **123**, 254502 (2019).

[3] A. Dörr, S. Hardt, H. Masoud, and H. A. Stone, Drag and diffusion coefficients of a spherical particle attached to a fluid–fluid interface, Journal of Fluid Mechanics **790**, 607 (2016).

[4] M. O'neill and K. Stewartson, On the slow motion of a sphere parallel to a nearby plan, Journal of Fluid Mechanics **27**, 705 (1967).

[5] J. Jeans, *Mathematical Theory of Electricity and Magnetism*, 5th ed., Cambridge Library Collection - Physical Sciences (Cambridge University Press, 1908).